

RESEARCH ON MILLIMETER-WAVE RADIATION CHARACTERISTICS OF SOLID TARGET

Xi Chen* and Jianzhong Xu

School of Electronic Engineering and Optoelectronic Technology, Nanjing University of Science and Technology, Nanjing 210094, China

Abstract—Millimeter-wave (MMW) radiation characteristics of solid targets are very complicated, and this paper starts with the research on modeling and simulation of the simple solid metal target. On the basis of the optical property of MMW, the two-ray propagation (direct reflection and ground secondary reflection of the solid target surface) is analyzed by means of the ray tracing theory in the geometrical optics, the radiation temperature calculation model is established. Furthermore, in combination with the panel-method-based geometric model and in accordance with the spatial analytic geometry and vector algebra theory, model calculation of the intersection movement between the radiometer and the target is analyzed and the MATLAB simulation platform for MMW radiation characteristics of the solid target is built. Under the assumed simulation conditions, simulation experiments on three types of solid metal targets (sphere, cylinder and cone) are performed to verify the proposed method in this paper. Meanwhile, comparative analysis between the MMW radiation characteristics of the circular metallic plate and those of the metallic ball with the same radius indicates that the spherical metallic target is equivalent to the non-ideal metallic circular planar target which is increased about 1.3 times in the linear size, and the result is validated through the measured data, which provides more accurate and effective data and theoretical support for target recognition and location in the millimeter-wave passive detection.

1. INTRODUCTION

With the development of MMW passive detection technology, MMW radiation characteristics of targets have become significant in the

Received 7 January 2013, Accepted 22 February 2013, Scheduled 22 February 2013

* Corresponding author: Xi Chen (10cx14@163.com).

research of target characteristics. For different objects, their capacities in emission, absorption and scattering of electromagnetic radiation within the MMW waveband are different; the characteristic information of the MMW radiation can be obtained through receiving the thermal radiation energy of objects by the high-sensitivity MMW radiometer [1,2]. The research on MMW radiation characteristics of the targets has played an important role in many fields, such as weapon system development, battlefield reconnaissance, range testing, stealth technology [3–6].

At present, the research on MMW radiation characteristics focuses mainly on the radiation measurement of metal targets on the ground using the missile-borne or airborne MMW radiometer, acquisition of the orientation, the size and the geometric center of the target and other information through one-dimensional waveform characteristics including amplitude, rise time, duration time, frequency, etc., and achievement of the target identification and localization. For example, Shi et al. [7] have analyzed the MMW (94 GHz) radiation temperature of the armored target on the ground, and studied the passive MMW stealth technology based on control of MMW radiation characteristics. Zhang and Zhao [8] have studied differences of MMW radiation characteristics between the tank and major interferences at the 8 mm waveband as well as the target identification method. However, the measured metal targets were approximated as planar targets in previous studies, so totally reflected sky brightness temperature of the targets can be applied to analysis and modeling of the antenna temperature. While the measured objects such as tanks and armored vehicles are three-dimensional targets in the practical application, their complex structure and different heights make the environment radiation temperature contribute differently to target radiation characteristics, therefore there is a certain error between the analysis result based on the current theoretical calculation model and the actual measurement result. Additionally, there is scarce reference literature on MMW radiation characteristics of the solid targets, and it is still the main means to obtain more accurate and effective target radiation characteristics through field radiation measurement experiments, for example, in Reference [9], the static radiation temperature values of several metal solid targets with regular shape were obtained through the actual measuring experiment, unfortunately no relatively detailed research was presented. But the measuring method is usually limited by the on-site conditions and the cost, so it is a more economical and convenient method to study MMW radiation characteristics of the solid targets through simulation with the aid of the powerful calculating ability of the computer.

In this paper, firstly, the modeling and simulation research on MMW radiation characteristics of simple metal solid targets are introduced, the radiation temperature model of the solid target is given, calculation of the intersection movement model between the radiometer and the target is analyzed, and the simulation procedure is presented. Secondly, simulation experiments on several solid metal targets with simple shapes are carried out by means of the above models, the comparative analysis between the obtained experimental result and the simulation result on the circular metal target is performed, the metallic spherical target is made to be equivalent to the non-ideal metallic circular planar target which is increased in the linear size so as to obtain a simple and direct method to estimate roughly MMW radiation characteristics of the solid metal target; finally, availability and feasibility of the method are verified through the actual MMW radiation measurement experiments.

2. MMW RADIATION MEASUREMENT PRINCIPLE

In the natural world, any object with a certain temperature is a radiation source, of which the radiation energy is usually characterized by the radiation temperature (or apparent temperature); when the physical temperature of an object is T_0 , the total radiation energy can be expressed as follows [10]:

$$T(\theta, \varphi) = \varepsilon T_0 + (1 - \varepsilon) T_s(\theta, \varphi) \quad (1)$$

where $T(\theta, \varphi)$ is the object radiation temperature in the direction (θ, φ) , including two portions (the radiant energy of the object itself and the reflected radiant energy from the surrounding environment); $T_s(\theta, \varphi)$ is the environment radiation temperature in the direction (θ, φ) ; ε is the emissivity of the object, and the reflectivity is $1 - \varepsilon$ according to Kirchhoff's law.

Within the millimeter-wave band, different targets have different radiation characteristics because they are diverse in geometric properties, dielectric properties etc.; therefore, the MMW passive detection and target recognition can be realized. When the target is scanned by the scanning beam of the radiometer antenna, the received MMW radiation power near the antenna can be expressed as the antenna temperature acquired in the radiation measurement [11], that is

$$T_A = \frac{1}{4\pi} \int_0^{2\pi} \int_0^\pi T(\theta, \varphi) G(\theta, \varphi) \sin \theta d\theta d\varphi \quad (2)$$

where $G(\theta, \varphi)$ is the radiation pattern of the antenna. It can be seen that from Equation (2), the antenna temperature distribution is the

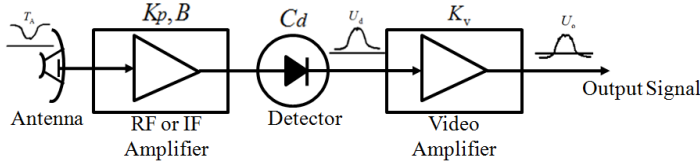


Figure 1. Schematic diagram of the radiometer.

weighted average of the product of the target radiation temperature and the antenna pattern, which serves as the smoothing method.

Because the radiation energy received by the radiometer antenna is very weak, so it needs to be amplified by the low noise amplifier at the front end of the receiver, and then be linearly transformed by the square-law detector into the output voltage signal proportional to the input noise power; at last, the one-dimensional output of target radiation measurement can be obtained [12] through filtering and further amplification of the video-frequency amplifier, the simplified functional block diagram of the radiometer is shown in Figure 1. So the final output voltage signal is expressed as follows:

$$U_o = K_v C_d K_p k B [T_A + T_e] \quad (3)$$

where K_v is the voltage gain of the video amplifier; C_d is the sensitivity of the square-law detector; B and K_p represent the equivalent bandwidth and the power gain before detection respectively; T_e is the system noise temperature of the receiver; k is the Boltzmann constant. All relevant parameters of the receiver circuit are invariable on the given detection conditions. Therefore, based on the one-dimensional output signal U_o in Equation (3), the signal waveform characteristics can be extracted so as to obtain useful target information. It is crucial to acquire the target radiation characteristics $T(\theta, \varphi)$ of the object in the complex environment.

3. CALCULATION MODEL

3.1. Calculation Model of Radiation Temperature

Compared with the planar targets, the geometric shapes of solid targets are very complicated; therefore, besides reflecting atmospheric radiation temperature in the observation direction from the upper surface of the target, the lateral surface of the target will produce multiple kinds of reflection by interacting with the surrounding environment, so the radiation propagation becomes fully complicated. Considering that the wavelength within the MMW waveband is small,

the energy is transferred by means of the bunching propagation in the space, which has the optical property, so the MMW radiation propagation can be analyzed through the ray tracing method in the geometrical optics [13]. In the MMW radiation measurement, there are numerous emission sources because any point on the target surface is a radiation source, so the reverse ray tracing is required to be used, which means that the receiving antenna of the radiometer is considered to be one radiation source, several rays emitted within the antenna beam range are tracked one by one. On the basis of the physical meaning of the radiation temperature, the radiation energy of each ray can be expressed as the target radiation temperature in this direction, and it does not change with the propagation path.

To simplify the analysis, a metal solid target is assumed to be placed on the smooth ground during the simulation and the model calculation, the surface of the target and background are the mirror reflection, and the diffraction effects can be ignored, so only the two-ray propagation (the target direct reflection and the ground secondary reflection) is taken into account. As shown in Figure 2, the plane XOY is the ground background, the point A represents the antenna of the detector, the metal solid target can be regarded as an ideal reflector, therefore the surface will reflect the environment radiation temperature in all directions, among which some rays irradiated on the target surface are directly reflected into the antenna, as shown in the solid-line path 1-1'. In the meantime, other rays are reflected by the target and reflected again by the ground background before entering the antenna, as shown in the dashed-line path 2-2'.

According to Equation (1), the emissivity of the metal target is $\varepsilon \approx 0$, the atmospheric radiation energy directly irradiating on the target surface will be completely reflected, so the radiation temperature can be approximately expressed as:

$$T_1(\theta, \varphi) = T_{\text{sky}}(\theta, \varphi) \quad (4)$$

where $T_{\text{sky}}(\theta, \varphi)$ is the sky brightness temperature.

For the secondary reflection ray, the sky brightness temperature reflected by the metal target surface firstly arrives at the ground, and then is reflected into the antenna through the smooth surface; meanwhile the radiation energy of the ground itself also enters into the antenna, so the radiation temperature can be expressed as:

$$T_2(\theta, \varphi) = \varepsilon_g T_g(\theta, \varphi) + (1 - \varepsilon_g) T_{\text{sky}}(\theta, \varphi) \quad (5)$$

where ε_g is the emissivity of the ground background and $T_g(\theta, \varphi)$ the ground background temperature.

Therefore, the total radiation energy received by the antenna is the weighted average of the radiation temperature of all rays within

on the target surface, the ray-tracing model is established by means of the line-plane intersection determining method. The ray path tracking schematic diagram of any micro element is shown in Figure 3, in which $O\text{-}XYZ$ is the geodetic coordinate system, the system does not change with movement of the detecting antenna and can be used to distinguish the different beam directions and point out the target location. The micro element S_i reflects the sky brightness temperature in the direction \vec{t} , and then the ray eventually enters the antenna along the direction \vec{r}_1 through different reflection paths in accordance with the vector relationship with the normal \vec{n} ; the vector \vec{t} , \vec{r}_1 and \vec{n} are located in the same plane, and the included angle of \vec{n} and \vec{t} is equal to that of \vec{n} and \vec{r}_1 . In the practical application, the reverse ray tracing path calculation is used.

Suppose the antenna A scans parallel to the Y axis at a horizontal speed of v , the position coordinate is $(x_a, y_a + vt_k, H)$ at t_k and H is the detecting height. The point A' is the mirror point of the point A relative to the XOY plane, so its position coordinate is $(x'_a, y'_a, z'_a) = (x_a, y_a + vt_k, -H)$. The straight line AM represents the detecting direction of the antenna, and the coordinate of the scanning point M on the ground is $(x_m, y_m, z_m) = (x_a, y_a + vt_k + H \tan \theta, 0)$, then the equation of the straight line $A'M$ can be expressed as:

$$\frac{x - x'_a}{x_m - x'_a} = \frac{y - y'_a}{y_m - y'_a} = \frac{z - z'_a}{z_m - z'_a} \quad (7)$$

Provided the coordinates of three vertices of the micro element respectively are $P_1(x_1, y_1, z_1)$, $P_2(x_2, y_2, z_2)$ and $P_3(x_3, y_3, z_3)$, in the reference coordinate system, so the plane equation of the micro element is $Ax + By + Cz + D = 0$, where

$$\begin{cases} A = y_1z_2 + z_1y_3 + y_2z_3 - z_2y_3 - z_3y_1 - z_1y_2 \\ B = -(x_1z_2 + z_1x_3 + x_2z_3 - z_2x_3 - z_3x_1 - z_1x_2) \\ C = x_1y_2 + y_1x_3 + x_2y_3 - y_2x_3 - y_3x_1 - y_1x_2 \\ D = -(Ax_1 + By_1 + Cz_1) \end{cases} \quad (8)$$

Through solution of Equations (7) and (8), the coordinate values of the intersection point G can be expressed as:

$$\begin{cases} x_g = k(x_m - x'_a) + x'_a \\ y_g = k(y_m - y'_a) + y'_a \\ z_g = k(z_m - z'_a) + z'_a \end{cases} \quad (9)$$

where $k = \frac{-(Ax'_a + By'_a + Cz'_a + D)}{A(x_m - x'_a) + B(y_m - y'_a) + C(z_m - z'_a)}$.

If the coordinates in Equation (9) lie within the coordinate range of the micro element as shown in Equation (10), the intersection point

G is validated; therefore the ray path can be determined to be the direct reflection or the secondary reflection.

$$\begin{cases} \min(x_1, x_2, x_3) < x_g < \max(x_1, x_2, x_3) \\ \min(y_1, y_2, y_3) < y_g < \max(y_1, y_2, y_3) \\ \min(z_1, z_2, z_3) < z_g < \max(z_1, z_2, z_3) \end{cases} \quad (10)$$

On the premise that the ray path is known, the included angle θ_T between the incident direction and the vertical axis is calculated according to the vector algebra and the space analytic geometry theory, so as to get the radiation temperature. The specific calculating method is presented as follows: the unit normal vector of the micro element S_i is defined as:

$$\vec{n}_0 = \{n_{0x}, n_{0y}, n_{0z}\} = \frac{1}{\sqrt{A^2 + B^2 + C^2}} \{A, B, C\} \quad (11)$$

The unit vector of the incident direction \vec{r} can be derived as follows:

$$\vec{r}_0 = \{r_{0x}, r_{0y}, r_{0z}\} = \frac{\{x_g - x_m, y_g - y_m, z_g - z_m\}}{\sqrt{(x_g - x_m)^2 + (y_g - y_m)^2 + (z_g - z_m)^2}} \quad (12)$$

Provided that the unit vector of the reflected direction \vec{t} is $\vec{t}_0 = \{t_{0x}, t_{0y}, t_{0z}\}$, then the relationship of \vec{t}_0 , \vec{r}_0 and \vec{n}_0 satisfies the expression $\vec{n}_0 = \frac{1}{|\vec{r}_0 + \vec{t}_0|} \cdot (\vec{r}_0 + \vec{t}_0)$, namely the equation set

$$\begin{cases} t_{0x}n_{0x} + t_{0y}n_{0y} + t_{0z}n_{0z} = r_{0x}n_{0x} + r_{0y}n_{0y} + r_{0z}n_{0z} \\ n_{0x}r_{0y}t_{0z} + n_{0y}r_{0z}t_{0x} + r_{0x}t_{0y}n_{0z} - n_{0z}r_{0y}t_{0x} \\ - r_{0z}t_{0y}n_{0x} - n_{0y}r_{0x}t_{0z} = 0 \\ t_{0x}^2 + t_{0y}^2 + t_{0z}^2 = 1 \end{cases} \quad (13)$$

Therefore, the direction cosines t_{0x} , t_{0y} and t_{0z} of the vector \vec{t}_0 can be obtained by solving Equation (13), those of the vector \vec{t} can be derived in a similar way. As per the definition of the direction cosine, the included angle between the vector \vec{t} and the vertical axis can be expressed as $\theta_T = \arccos(t_{0z})$, and then the final radiation temperature can be calculated in combination with Equations (4)–(6).

3.3. Simulation Procedure

The MATLAB simulation system of the metal solid targets' MMW radiation characteristics can be established through the following procedure:

Step 1: The triangle elements are divided by setting size and properties of the element in the ANSYS software, to build the

geometric model of the metal solid target and obtain the data of the micro elements and the corresponding node coordinates;

Step 2: The rays are evenly divided at the interval $\Delta\theta$ within the antenna beam range. For each ray, when the antenna position is $(x_a, y_a + vt_k, H)$ at t_k , the intersection point is calculated according to Equations (7)–(10) to get the ray-tracing path;

Step 3: For the known reflection path, the angle θ_T of the incident direction can be calculated as per Equations (11)–(13), which is substituted into Equations (4) and (5) to calculate the radiation temperature;

Step 4: By going through all ray-tracing path of the beam range by repeating Step (2) and Step (3), the total radiation temperature received by the antenna can be calculated as per Equation (6), which is substituted into Equation (2) to obtain the value of the antenna temperature at the moment t_k ;

Step 5: To determine the location coordinates of the antenna at the next moment $t_{k+1} = t_k + i\Delta t$, and repeat the calculation from Step (2) to Step (4), so as to get the curve of the antenna temperature during the intersection of the radiometer and the target. Finally, the one-dimensional output signal from millimeter-wave radiation measurement of the solid target can be obtained by using Equation (3).

4. SIMULATION AND ANALYSIS OF EXPERIMENTAL RESULTS

According to the above simulation procedure, the simulation programs are written in the MATLAB language. The simulation parameters are given as follows: the detection height is $H = 25$ m, the detection angle is $\theta_F = 30^\circ$, the beam width at -3 dB is $\theta_{3\text{dB}} = 1.8^\circ$, the ray-tracing interval is $\Delta\theta = 0.05^\circ$, the initial position coordinate of the horizontal scanning antenna is $(0, -20, 25)$, and the speed is $v = 1$ m/s, the time sampling interval is $\Delta t = 0.1$ s. The operating frequency of the radiometer is 94 GHz, the system bandwidth is $B = 6$ GHz, the power gain of the radio frequency amplifier is $K_p = 50$ dB, the voltage gain of the video amplifier is $K_v = 80$ dB, the detector sensitivity is $C_d = 800$ V/W, and the noise temperature of the system is $T_e = 1160$ K. The metal solid target is placed at the original point of the geodetic coordinate system. The clear sky brightness temperature in 3 mm waveband can be accessed from Reference [15], and the background radiation temperature curve of the concrete ground which changes with the observation angle is available in Reference [16].

Simulation 1: simulation experiments on three simple metal solid targets (ball, cylinder and cone) are performed, in which the radiuses

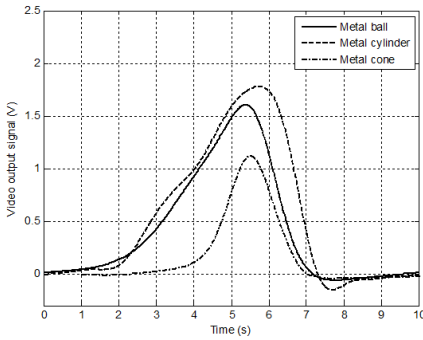


Figure 4. Simulated signal of three metal solid targets.

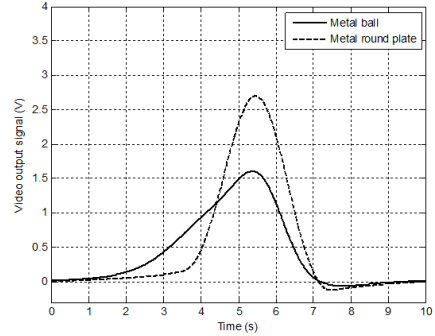


Figure 5. Simulation signal of metal ball and circular metal plate.

of the ball, the cylinder and the base radius of the cone are 1 m, and the height of the cylinder is 2 m as well as that of the cone. The output video voltage signal of the radiometer is shown in Figure 4.

Simulation 2: The radiation characteristic of the circular metal plate, which has the same radius as the metal ball, are analyzed by means of the simulation modeling method proposed in this paper. Then the output simulation signal is respectively compared with the output signal of the metal ball and the theoretical calculation signal of the circular metal plate, as shown in Figures 5 and 6. Notice that the simulation results given here are the output voltage signal of the antenna temperature contrast which is reversely amplified.

From the above figures, it can be concluded that:

(1) When the short-range detection of the simple metal solid objects on the ground is carried out through the millimeter-wave radiometer, the radiation output signals of the solid targets with the similar size and different geometry shapes are different. It can be seen from Figure 4, the signal peak of the cylinder is slightly higher than that of the ball, and both of them are much higher than that of the cone. Because the upper plane of the cylinder mainly reflects the sky brightness temperature, the weighted radiation temperature near the signal peak decreases (while the antenna temperature contrast increases), so the signal peak of the cylinder is the highest. Since the background radiation temperature of the ground makes great contributions to the antenna temperature based on the spatial relationship between the inclined lateral surface of the cone and the detection beam, the signal peak of the cone is relatively low. Meanwhile, from comparison of the pulse width of the output signals, they are similar for the ball and the cylinder, but that of the cone

is relatively narrow, because the geometric sectional area of the cone becomes gradually smaller from its bottom to the top. It is illustrated that the MMW radiation characteristics of the metal solid targets can show differences in their structural characteristics.

(2) To further describe the MMW radiation characteristics of the solid targets, the metal ball target is taken as an example, compared with the output radiation signal of the circular metal plate with the same linear size, the output signal waveform of the metal ball changes on the same detection conditions and the signal peak decreases by approximately 40%, but the half-peak width is broadened about 1.3 times. It means that, the different parts of the solid target will produce the secondary-reflection radiation temperature through the ground in addition to direct reflection of the sky brightness temperature, because the solid target has a certain height; furthermore, the radiation temperature of the ground background and the sky brightness temperature of other incident angles are higher than the sky brightness temperature of the zenith angle; therefore, the antenna temperature contrast (absolute value) of the solid target will decrease, namely, the peak of the output signal is smaller than the signal peak of the planar target. At the same time, the spot area created by the antenna beam on the ground is fixed for a given detection height, so widening of the waveform width can be understood as the radiation detection is from the planar targets on the ground which become larger in size. For this reason, the radiation output of the circular metal plate is considered to be the reference standard, and the metal ball can be expressed as a equivalent non-ideal metallic circular planar target which is increased by about 1.3 times in the linear size, so as to approximately estimate its radiation characteristics by means of the theoretical model of the planar metal target.

(3) Compared to the output signal obtained through the theoretical calculation model of the MMW radiation detection in the planar metal target on the ground, the output signal waveform of circular metal plate acquired by means of the proposed simulation method is basically consistent. It is concluded that the modeling and simulation method of the MMW radiation characteristics of the solid target can also be applied to a planar target, which can be regarded as a special case, so the proposed method is verified.

In order to validate further the feasibility of the proposed method, the on-site scale-down experiment is performed, in which the radius (80 mm) of the metal ball is same as that of the circular metal plate, the detection height is 2 m, and other parameters remain consistent with those in the simulation experiment. The actual measurement result is shown in Figure 7. It can be seen from Figures 5 and 7, compared with

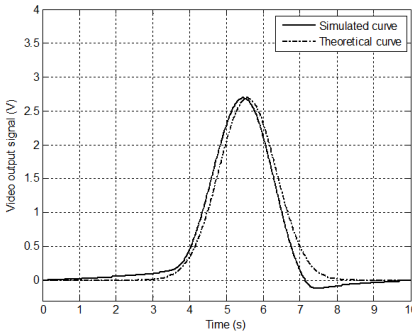


Figure 6. Simulation signal and theoretical signal of circular metal plate.

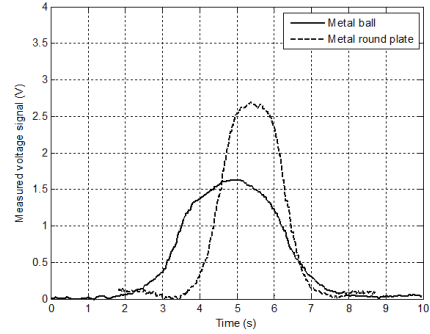


Figure 7. Measured signal of metal ball and circular metal plate.

the actual output signal through the target radiation measurement, the output signal obtained by the proposed simulation method has the similar waveform; and two main waveform characteristic parameters (the peak value and the pulse width) of the output signal are identical with the measured data on the whole, which can accord with the measured results well. Therefore, the MMW radiation characteristics model of the solid target established through the simulation method in this paper can provide more convenient and effective data support for the field tests.

5. CONCLUSION

The study of MMW radiation characteristics of the solid targets has an important application value; this paper starts from modeling and simulation of the simple solid target. The ray tracing theory is used to analyze the two-ray radiation propagation (direct reflection and ground secondary reflection) on the surface of the solid target, the calculation model of the radiation temperature is established; and according to the geometric model subject to division of triangle surface element of the metal ball and the spatial geometrical relationship of the intersection movement between the detector and the target, the MATLAB simulation platform of MMW radiation characteristics of the metal solid target is achieved. On this basis, simulation experiments on several simple solid targets and circular metal plate are performed, the results show that the metal ball can be equivalent to a non-ideal metallic circular planar target which is enlarged about 1.3 times in the linear size; the simulation results are identical with the measured results, through which the correctness and feasibility of the proposed method is verified. It can provide more convenient and

accurate experimental data for the field tests, and theoretical support for location of millimeter-wave passive detection and recognition as well as development of the millimeter-wave passive detection system.

Because the MMW radiation characteristics are affected by many complicated factors in the actual background, modeling and analysis of MMW radiation characteristics of simple solid targets only are performed in this paper on the given detection conditions so as to facilitate the research. However, for the real solid targets with complex structure such as tanks and armored vehicles, computational accuracy will become worse if the method is used; under the circumstances, it needs to analyze the propagation process with many times of reflections and diffractions by means of the multiple ray tracing method on the basis of the two-ray radiation propagation model, so as to calculate the radiation temperature and implement intensive study in the future.

ACKNOWLEDGMENT

This work is partially supported by the China Postdoctoral Science Foundation Funded Project (No. 20100481151), and the NUST Research Funding (No. 2011YBXM73). The authors also gratefully acknowledge the helpful comments and suggestions of the reviewers, which have improved the presentation.

REFERENCES

1. Hu, T. Y., Z. L. Xiao, J. Z. Xu, and L. Wu, "Effects of reverse radiation noise on millimeter-wave radiometric imaging at short range," *Progress In Electromagnetics Research M*, Vol. 21, 177–188, 2011.
2. Chen, X. and J.-Z. Xu, "A novel method for waveform jamming based on millimeter-wave alternating current radiometer," *Journal of Electromagnetic Waves and Applications*, Vol. 27, No. 1, 1–11, 2013.
3. Guo, R., R. Z. Liu, J. Zhang, and G. Li, "Study on damage assessment of terminal-sensitive projectile firing at armored targets," *2011 Fourth International Conference on Information and Computing*, 302–305, 2011.
4. Li, X., Z. M. Dong, H. Wang, Q. C. Meng, Z. T. Wang, and Y. W. Zhang, "A novel approach to selecting contractor in agent-based multi-sensor battlefield reconnaissance simulation," *International Journal of Computational Intelligence Systems*, Vol. 5, No. 6, 985–995, 2012.

5. Demirci, S., H. Cetinkaya, E. Yigit, C. Ozdemir, and A. A. Vertiy, "A study on millimeter-wave imaging of concealed objects: Application using back-projection algorithm," *Progress In Electromagnetics Research*, Vol. 128, 457–477, 2012.
6. Zhang, G. F., G. W. Lou, and X. G. Li, "Experimental research on passive millimeter wave radiometric stealth technology of metal objects," *J. Infrared Millim. Terahz Waves*, Vol. 33, No. 12, 1239–1249, 2012.
7. Shi, X., G. W. Lou, X. G. Li, G. F. Zhang, and J. Y. Nie, "Modelling and calculating of millimeter wave radiant temperature for armored target," *J. Infrared Millim. Waves*, Vol. 26, No. 1, 43–46, 2007 (in Chinese).
8. Zhang, Y. M. and Z. B. Zhao, "Techniques of 8 mm wave band signal detection and identification for tank," *J. Infrared Millim. Waves*, Vol. 28, No. 3, 177–180, 2009 (in Chinese).
9. Zhang, C., "Study on 3 mm band target radiation characteristics," MS Thesis, Nanjing University of Science and Technology, Nanjing, China, 2008 (in Chinese).
10. Zhang, Z. Y. and S. J. Lin, *Microwave Radiometry and Its Application*, Publishing House of Electronic Industry, Beijing, 1995.
11. Kaste, O. C., "The comparison of signal and noise value with measurement value about 35 GHz passive radiometer," *AD-A 040366*, 16–24, 1980.
12. Li, X. G. and Y. H. Li, *Foundation of MMW Proximity Technique*, Beijing Institute of Technology Press, Beijing, 2009.
13. Sarker, M. S., A. W. Reza, and K. Dimyati, "A novel ray-tracing technique for indoor radio signal prediction," *Journal of Electromagnetic Waves and Applications*, Vol. 25, Nos. 8–9, 1179–1190, 2011.
14. Stolarski, T., Y. Nakasone, and S. Yoshimoto, *Engineering Analysis with ANSYS Software*, Butterworth Heinemann, UK, 2007.
15. Lu, X., Z. L. Xiao, L. Wu, and J. Z. Xu, "A novel estimation of MMW sky brightness temperature based on BP neural network," *Cross Strait Quad-Regional Radio Science and Wireless Technology Conference*, Vol. 1, 230–233, Jul. 2011.
16. Fan, X., Q. H. Ma, Y. C. Zhao, and Z. Lu, "The goodness of fit modeling on millimeter wave radiation brightness temperature signal of background," *Guidance and Fuze*, Vol. 30, No. 3, 41–45, 55, 2009 (in Chinese).